

On the Reduction of the Spherical Point-in-Polygon Problem for Antipode-Excluding Spherical Polygons

Ziqiang Li^{1,*} and Jindi Sun²

¹Department of Mathematics, Virginia Polytechnic Institute and State University,
Blacksburg, VA 24061

²Department of Biomedical Engineering, University of Arizona, Tucson, AZ 85721

*Communicating author: zqli@vt.edu

September 7, 2023

Abstract

Spherical polygons used in practice are nice, but the spherical point-in-polygon problem (SPiP) has long eluded solutions based on the winding number (**wn**). That a punctured sphere is simply connected is to blame. As a workaround, we prove that requiring the boundary of a spherical polygon to never intersect its antipode is sufficient to reduce its SPiP problem to the planar, point-in-polygon (PiP) problem, whose state-of-the-art solution uses **wn** and does not utilize known interior points (KIP). We refer to such spherical polygons as boundary antipode-excluding (BAE) and show that all spherical polygons fully contained within an open hemisphere is BAE. We document two successful reduction methods, one based on rotation and the other on shearing, and address a common concern. Both reduction algorithms, when combined with a **wn**-PiP algorithm, solve SPiP correctly and efficiently for BAE spherical polygons. The MATLAB code provided demonstrates scenarios that are problematic for previous work.

Contents

1	Statements	2
2	Practical notion of small spherical n -gons	5
3	Reduction Algorithms and Homotopy	7
4	Implementation	12
5	Test cases	12
6	Discussion	17
A	Code Listings	20

1 Statements

A spherical polygon is a region on a sphere bounded by arcs of great circles.

Suppose G is a spherical polygon on the unit sphere S^2 with an orientable boundary ∂G . Given any test point $Q \in S^2$, we decide on one outcome among $Q \in \partial G$, $Q \in \overset{\circ}{G}$, or $Q \notin G$; namely, is Q on the boundary, in the interior, or in the exterior of G ?

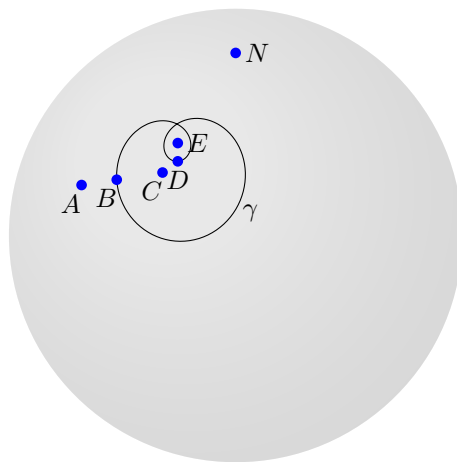


Figure 1: More generally, let S^2 be the unit sphere, N be the north pole, and $\gamma \subset S^2$ be the depicted non-simple loop with N in the exterior. Then A is in the exterior, B, D are on the boundary, and C, E are in the interior.

In comparison, the point-in-polygon (PiP) problem is stated as follows. Suppose G' is a polygon in \mathbb{E}^2 with an orientable boundary $\partial G'$. Without loss of generality, let the origin $O \in \mathbb{E}^2$ be the test point. We decide on one outcome among $O \in \partial G'$, $O \in \overset{\circ}{G}'$, or $O \notin G'$, *i.e.*, is the origin on the boundary, in the interior, or in the exterior of G' ?

As the title suggests, we seek a sufficient condition for a spherical polygon so that its SPiP-outcome is decided based on both the PiP-outcome and said condition.

1.1 Review

Humanity thrives on the round Earth and makes important decisions on its surface. A type of question we frequently answer is: Is this point Q inside this region $\Omega \subset S^2$ specified by its boundary $\gamma = \partial\Omega$? Developing a reliable spherical point-inclusion test is thus crucial to geographic information systems (GIS) and numerical simulation on spheres (Li and Aryana, 2018; Li, 2023) but sporadic attention has been given to it. Given that Ω is typically approximated and preserved digitally as a spherical n -gon G , we have the spherical point-in-polygon (SPiP) problem.

The earliest known crossing-number (**cn**) algorithm for SPiP with simple boundary is proposed in Bevis and Chatelain (1989). Their algorithm uses a known interior point (KIP) $P \in \overset{\circ}{G}$, *i.e.*, P is known *a priori* to be an interior point of G . During the test, the unique arc of great circle PQ intersects each side of G , and each intersection counting towards **cn** as one crossing. The odd-even parity of **cn** is used to discriminate between $Q \in \overset{\circ}{G}$ and $Q \notin G$. However, this method offers two rooms for improvement. First, the algorithm fails when the arc \widehat{PQ} is not well-defined, thereby requiring a second KIP. Secondly and more dramatically, when Q lies on the extension of any side of G , it is unclear how the intersection should count towards **cn**.

Recent progress addressing both issues is documented in Ketzner et al. (2022). Again, based on the crossing number (**cn**) and one known interior point $P \in \overset{\circ}{G}$, their algorithm computes for each vertex of G an azimuthal angle relative to P , and all test points will be handled by intersecting \widehat{PQ} with G in the P -north, rotated coordinate system. Their algorithm removed the extension restriction on Q .

So far, no formulation has been provided based on the winding number **wn** of ∂G around Q . The (in)-convenient fact that “a punctured sphere is

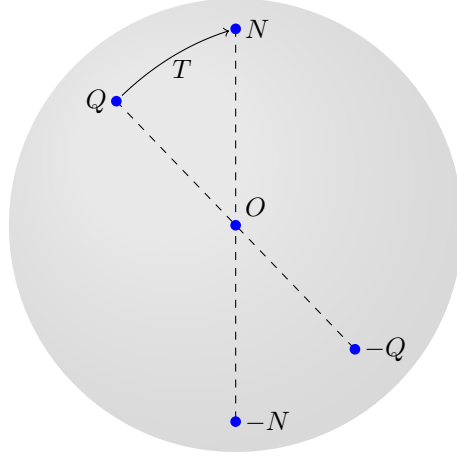


Figure 2: The Q -north coordinate system can be produced by rotating Q along \widehat{QN} to N . This rotation induces a linear transformation T . If Q is the south pole, any 180° rotation would suffice.

simply connected” is to blame, *i.e.*, $\pi_1(S^2 \setminus \{N\})$ is a trivial fundamental group. It must be acknowledged that **cn** and **wn** result in different notions of interiority, with the **wn** being more consistent and conceptually elegant with several authors lobbying for their preference over **cn**, such as (Sunday, 2021) and the authors of this paper. We make no further comment on their distinctions.

1.2 Winding number

Winding number (**wn**) is intuitively defined as the number of times a loop γ in the Euclidean plane \mathbb{E}^2 wraps around a non-boundary test point, *e.g.*, $O \in \mathbb{E}^2$ in a conventional direction. In algebraic topology, we may define “completion of a counterclockwise loop around the test point” to be the generating equivalence class $[l] \in \pi_1(S^2 \setminus \{O\})$ in the fundamental group $\pi_1(S^2 \setminus \{O\}) \cong \mathbb{Z}$, thereby establishing that $[l]^{\mathbf{wn}} = [\gamma]$. The **wn** is usually calculated by

$$\mathbf{wn} = \frac{1}{2\pi} \oint_{\gamma} d\theta = \frac{1}{2\pi} \sum_{i=1}^n \Delta\theta_i, \quad (1)$$

where $\theta(x)$ is the polar coordinate of a point $x \in \gamma$ and the summation is for any polygon that is homotopic to γ . In practical computer algorithms, **wn** is

computed using a crossing test (refer to Sunday (2021)) which is significantly faster than summing up the signed angles $\Delta\theta_i$, ($i = 1, \dots, n$) spanned by each side of the polygon, which requires the use of inverse trigonometric functions.

1.3 Spherical polygons

In general, a spherical polygon need not be convex, its boundaries intersect or even overlap with itself, and its sides may be larger than a semicircle. Under practical circumstances, spherical polygons are restricted to be convex, simple, with each side less than a semicircle. Any contiguous part of any country on Earth is fully contained within an open hemisphere. Spherical triangulations uses spherical triangles where dyadic refinement keeps subdividing spherical triangles into having exponentially smaller area (Baumgardner and Frederickson, 1985). It is thus important to investigate criteria for small spherical polygons that will facilitate a **wn**-SPiP algorithm that fully utilizes a PiP algorithm as a subroutine.

2 Practical notion of small spherical n -gons

Assuming $Q \notin \partial G$, we first deal with $\pi_1(S^2 \setminus \{Q\}) \cong \{0\}$. Noting that $\pi_1(S^2 \setminus \{\pm Q\}) \cong \mathbb{Z}$, we seek a sufficiently general property of G such that whenever $\pm Q \notin G$, the reduction algorithm would identify PiP-outcomes as SPiP-outcomes. This would isolate $\pm Q \in G$ for further discrimination. We thus explore antipode-exclusion criteria for G , where the basic premise is to assert that $-Q \in G$ implies $Q \notin G$. Suppose $G \subset S^2$ is a spherical polygon and $Q \in S^2$ is a test point.

Definition 2.1 (Antipode). The mirror image of Q across the center of S^2 is called the antipode of Q and written as $-Q$.

Definition 2.2 (Antipode Exclusion). G satisfies the antipode-excluding (AE) property if whenever $Q \in G$, its antipode $-Q \notin G$.

Definition 2.3 (Boundary AE). G satisfies the boundary antipode-excluding (BAE) property if whenever $Q \in \partial G$, its antipode $-Q \notin \partial G$.

Remark 2.4. The AE property of G is equivalent to $G \cap -G = \emptyset$. The BAE property is equivalent to $\partial G \cap (-\partial G) = \emptyset$. By definition, AE implies BAE.

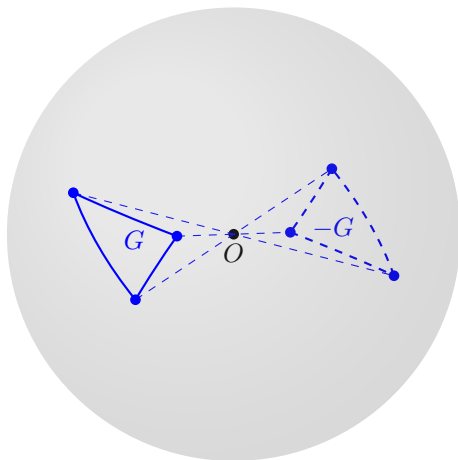


Figure 3: An example of an AE spherical triangle polygon G which does not intersect its antipode $-G$. G is further BAE. G is significantly less than an open hemisphere in terms of area. $\pm G$ occupy antipodal open hemispheres.

A BAE spherical polygon G is practical in the sense that it allows the following discrimination between $\pm Q \in \partial G$:

- If it is further determined that $Q \in \partial G$, halt.
- If it is further determined that $-Q \in \partial G$, declare that $Q \notin G$.

Therefore, a robust SPiP algorithm for BAE spherical polygons would first discriminate $\pm Q \in \partial G$ and then perform PiP on a **wn**-preserved polygonal projection $G' \subset \mathbb{E}^2 \setminus \{O\}$ of $G \approx \gamma \subset S^2 \setminus \{\pm Q\}$ onto \mathbb{E}^2 . Before we develop such an algorithm, we focus on an even more practical notion for small spherical polygons.

Definition 2.5 (Containment by Open Hemisphere). Let $G \subset S^2$ be a spherical polygon. Suppose G is containable in an open hemisphere. Then we say that G hemisphere-contained (HC).

Proposition 2.6 (HC \implies AE \implies BAE). Let $G \subset S^2$ be a HC spherical polygon. Then G is AE and further BAE.

For proof, we note that all antipodes of an open hemisphere are exterior to it, so any closed subset of an open hemisphere is certainly also AE. For an end-user, algorithms for BAE spherical polygons are directly applicable to

hemisphere-contained spherical polygons which describes the most common use case. We conclude this section with two conveniences. The first removes sides that are too long from consideration, which justifies conventional restrictions on the length of arcs (Todhunter, 1886, §1, Art. 4, p. 2).

Corollary 2.7. Let $G \subset S^2$ be a BAE spherical polygon. Then all sides of G are less than a semicircle.

Proof. By contradiction. Suppose G contains a side at least as large as a semicircle, then this side, which is closed, must contain a closed semicircle, which has antipodal endpoints. \square

The second convenience is a straightforward discrimination algorithm upon $\pm Q \in \partial G$. This occurs when the PiP-outcome is $O \in \partial G'$, and is handled by Proposition 2.8. Various proofs are left to the reader with a sketch provided as Figure 4.

Proposition 2.8 (Disambiguation). Let $AB \subset S^2$ be an arc of great circle less than a semicircle, and let $Q \in S^2$ be a point. Suppose arc AB intersects the straight line uniquely determined by $\pm Q$, then the midpoint M of the chord AB is in the same (*resp.*, antipodal) open hemisphere centered at $\pm Q$ if $\angle MOQ$ is acute or zero (*resp.*, is obtuse or flat).

3 Reduction Algorithms and Homotopy

Given a test point $Q \in S^2$ and a boundary $\gamma = \partial G \subset S^2$, this section provides an overview of the SPiP-to-PiP reduction algorithm when $\pm Q \notin \gamma$. The main idea is to project S^2 onto some plane such that the concept of winding (in this case, homotopy classes, **wn**) is preserved. We first acknowledge that winding breaks down upon $\pm Q \in \gamma$, but it is caught by Proposition 2.8. In the footsteps Bevis and Chatelain (1989) and Ketzner et al. (2022), we first investigate the Q -north rotation of S^2 , *i.e.*, rotating S^2 such that Q becomes the north pole. We then go off the beaten track and illustrate why an alternative shearing-based projection fails to preserve **wn**.

3.1 Rotation-based projection

The technical part of our SPiP algorithm is fully outsourced to PiP algorithms thanks to the following maneuver. Let $[x_i, y_i, z_i]^T \in \mathbb{E}^3$ be the Cartesian coordinates of the vertices v_i , $i = 1, \dots, n$, where v_i are successive vertices

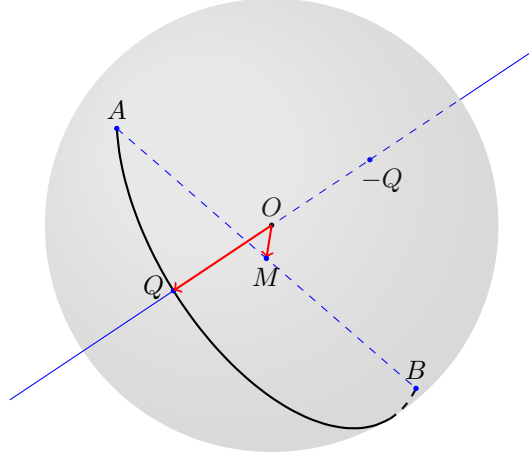


Figure 4: Visualization of Proposition 2.8 when Q lies on the arc AB where AB is smaller than a semicircle. The midpoint M of the chord AB must then be closer to Q than $-Q$. Exchange the labels $\pm Q$ to visualize the other case, where $-Q$ lies on the arc AB and M must be closer to $-Q$ than Q .

of the spherical n -gon $G \subset S^2$. Let (θ, ϕ) describe the polar angle $\theta \in [0, \pi]$ and the azimuthal angle $\phi \in \mathbb{R}$ of the test point Q . For ease of discussion, let N and $-N$ be the north and south pole, respectively. Remember that this part of the algorithm is executed with the assertion that $\pm Q \notin G$ in mind.

We perform a rotation of S^2 along the arc QN such that Q becomes N . (This rotation is trivial if $Q = S$.) This rotation induces a linear transformation $T : \mathbb{E}^3 \rightarrow \mathbb{E}^3$ on the Cartesian coordinates of points on S^2 , *i.e.*, $T([x_i, y_i, z_i]^\top) = \mathbf{R}[x_i, y_i, z_i]^\top = [x'_i, y'_i, z'_i]^\top$, where $\mathbf{R} \in SU(3)$ is a rotation matrix. Because $\pm Q \notin G$, we see that $T(\pm Q) = \pm N \notin T(G)$. We then project the rotated coordinates onto the Euclidean plane \mathbb{E}^2 by $\pi : \mathbb{E}^3 \rightarrow \mathbb{E}^2$, $[x'_i, y'_i, z'_i]^\top \mapsto [x'_i, y'_i]^\top$, noting that $[x'_i, y'_i]^\top \neq O$ is guaranteed. We thus claim the following reduction.

Proposition 3.1 (Rotation-based reduction). Let $G \subset S^2$ be a BAE spherical polygon with vertices v_1, \dots, v_n . Suppose $Q \in S^2$ is not a boundary point of G . Then the outcome of **wn**-SPiP for G around Q (*i.e.*, $Q \in \partial G$, $Q \in \overset{\circ}{G}$, $Q \notin G$) is identical to the outcome of **wn**-PiP for the polygon G' with vertices $(\pi \circ T)(v_i)$, $i = 1, \dots, n$ around O (*i.e.*, $O \in \partial G'$, $O \in \overset{\circ}{G}'$, $O \notin G'$).

Proof. We show through construction that π preserves **wn** from $S^2 \setminus \{\pm N\}$

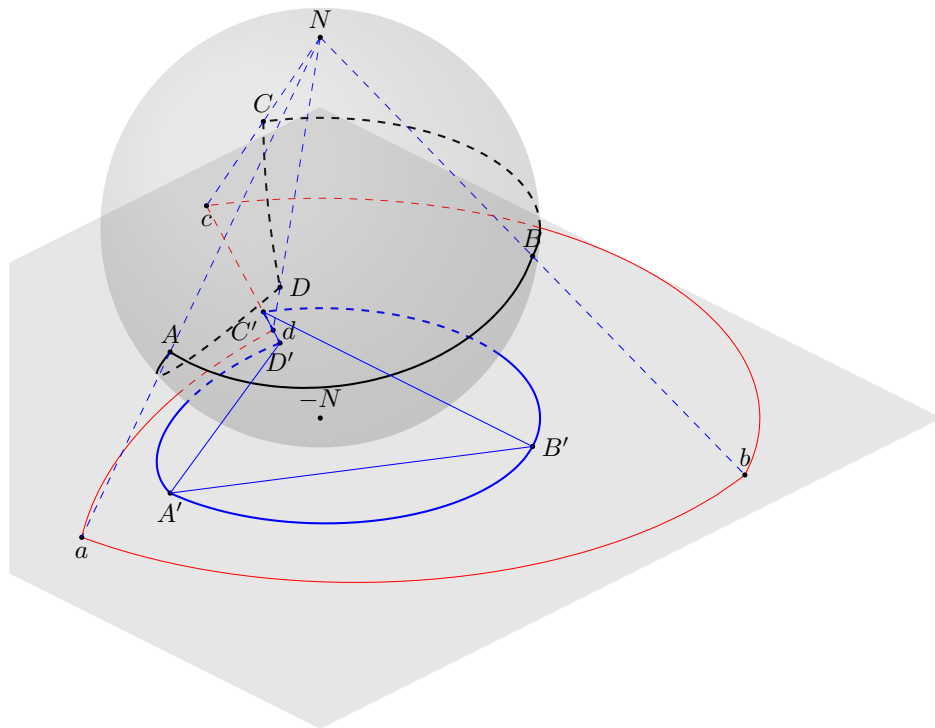


Figure 5: The projection π preserves homotopy classes between $\pi_1(S^2 \setminus \{\pm N\})$ and $\pi_1(D^2 \setminus \{O\})$. The south-polar stereographic projection of G is depicted as the loop $abcda$. Note that N is on the great circle determined by \widehat{CD} , so both cd and $C'D'$ are straight line segments that are collinear with $-N$.

to $D^2 \setminus \{O\}$, where D^2 is the closed unit disk.

Let $\tau : S^2 \setminus \{-N\} \rightarrow \mathbb{E}^2$ be the south-polar stereographic projection (specified by Snyder (1987, p. 158) but with different coordinates)

$$\tau([x, y, z]^\top) = (2 \cot \frac{\theta}{2})[x, y]^\top, \quad (2)$$

then $S^2 \setminus \{\pm N\}$ is homeomorphic to $E^2 \setminus \{O\}$ under τ . Then note that $D^2 \setminus \{O\} \subset \mathbb{E}^2 \setminus \{O\}$, and $f_t : [x, y]^\top \mapsto (1 + (2 \cot \frac{\theta}{2} - 1)t)[x, y]^\top$, ($t \in [0, 1]$) is a homotopy between $\pi(T(G))$ and $\tau(T(G))$.

Most importantly, if an edge $\tau(v_i)\tau(v_j) \in G'$ contain O , then both $\tau(\widehat{v_i v_j})$ and $\pi(\widehat{v_i v_j})$ are line segments because τ projects longitudinal lines onto straight lines. And so, $\tau(\widehat{v_i v_j}) = \tau(v_i)\tau(v_j)$. Otherwise, if an edge $\tau(v_i)\tau(v_j)$ does not contain O , then the region Ω_i bounded by $\tau(v_i)\tau(v_j)$ and $\tau(\widehat{v_i v_j})$ has a simply connected preimage under τ , implying that $O \notin \Omega_i$. This paragraph proved that G and G' are in identified equivalence classes in $\pi_1(S^2 \setminus \{\pm Q\}) \cong \pi_1(D^2 \setminus \{O\})$. \square

The reader is reminded that] the specific choice of τ and π are significant but not necessary unique. Note, also, that S^1 is a contraction of both $S^2 \setminus \{\pm Q\}$ and $D^2 \setminus \{O\}$ so the two spaces must be homotopic (Hatcher, 2001).

3.2 Shearing-based projection

Out of curiosity, we explored what would happen if the axis $\pm Q$ is made parallel to the $+z$ -axis not through a rotation but through shearing. After all, Q -north rotation is not the only way to align the Q -axis with a coordinate axis. In fact, the Q -axis could be aligned with its closest coordinate axis through transformations T_x , T_y , and T_z . Given $Q(a, b, c)$ in Cartesian coordinates, this choice is made as follows: If $|a|$ is the largest among $|a|$, $|b|$, and $|c|$, then T_x aligns the Q -axis with the x -axis. Or, if $|b|$ is the largest, then T_y aligns the Q -axis with the y -axis. Or, if $|c|$ is the largest, then T_z aligns the Q -axis with the z -axis. We define the shearing transformations as:

$$T_x(x, y, z) = (x, y - \frac{b}{a}x, z - \frac{c}{a}x), \quad (3)$$

$$T_y(x, y, z) = (x - \frac{a}{b}y, y, z - \frac{c}{b}y), \quad (4)$$

$$T_z(x, y, z) = (x - \frac{a}{c}z, y - \frac{b}{c}z, z). \quad (5)$$

Note that the denominators a , b , and c are never zero when used because

$$(\max\{|a|, |b|, |c|\})^2 = \max\{a^2, b^2, c^2\} \geq \frac{a^2 + b^2 + c^2}{3} = \frac{1}{3}. \quad (6)$$

Regardless of the shearing, let (x', y', z') be the transformed coordinates.

- If T_x is used, we feed (y', z') or (z', y') into PiP if $a > 0$ or $a < 0$.
- If T_y is used, we feed (z', x') or (x', z') into PiP if $b > 0$ or $b < 0$.
- If T_z is used, we feed (x', y') or (y', x') into PiP if $c > 0$ or $c < 0$.

The transposition of coordinates is necessary to account for orientation changes due to the projection operation; otherwise, the result of the PiP algorithm is exactly opposite of the desired. The disambiguation of Q and an offending side $v_i v_j$ is settled using Proposition 2.8, by checking if $\overrightarrow{OQ} \cdot \overrightarrow{OM} > 0$, where M is the midpoint of $v_i v_j$. Note that Line 10 of Algorithm 1 is a special case of this test. This alternative algorithm is noted in Algorithm 2, and we move to justify its correctness.

Let $\widehat{AB} \in S^2$ be a side of a BAE spherical polygon G , $\pi \circ T_d$ be the shearing-based projection in use (with $d = x, y, z$). Further let $A' = (\pi \circ T)(A)$ and $B' = (\pi \circ T)(B)$ be the projected points, $A'B'$ be a side of polygon G' , and $\widehat{A'B'} = (\pi \circ T)(\widehat{AB})$ be the projection of the arc \widehat{AB} . Note that $\widehat{A'B'}$ is a curve segment and not necessarily an arc, despite our choice of notation.

Proposition 3.2 (Longitude-to-line). $O \in A'B'$ if and only if $Q \in \widehat{AB}$.

Proof. Assume that $Q \in \widehat{AB}$. Then OAB determines a plane α and $(\pi \circ T_d)(\alpha)$ contains the d -axis. The projection of $(\pi \circ T_d)(\alpha)$ onto the coordinate plane perpendicular to the d -axis is a line, so O is collinear with $A'B'$. To show that $O \in A'B'$, repeat the same argument with $Q \in \widehat{AQ}$ and $Q \in \widehat{BQ}$, obtaining that O is collinear with $A'O$ and $B'O$, hence $O \in A'B'$.

In the reverse direction, note that the steps above are reversible, especially note that the intersection of a plane with a sphere is an arc of great circle. \square

Proposition 3.3 (Homotopy preservation). The region $R \subset \mathbb{E}^2$ bounded by $A'B'$ and $\widehat{A'B'}$ does not contain O in its interior.

Proof. By contradiction. Assume that $O \in \overset{\circ}{R}$. Then extend $A'O$ to intersect $\widehat{A'B'}$ at C' . Because $C' \in A'B'$, there exists $C \in \widehat{AB}$ with C' as its projection. Because $O \in A'C'$, we know that $Q \in \widehat{AC} \subset \widehat{AB}$, forcing $O \in A'B'$, so $O \in \partial R$. \square

The two propositions above confirm that shearing-based reduction preserves homotopy classes before and after $\pi \circ T_d$, just like rotation-based reduction.

4 Implementation

Our proposed rotation-based reduction algorithm is listed in Algorithm 1, which calls the modified PiP algorithm listed in Algorithm 3. Note that the PiP algorithm by Sunday (2021) is easily modified to detect $O \in \partial G'$, which is crucial for the AE-based Algorithm 1. As such, we incorporated a test for boundary points, which may be relaxed in practice to account for floating-point arithmetic.

Our alternative, shearing-based algorithm is listed in Algorithm 2, which also calls the modified PiP algorithm listed in Algorithm 3.

Finally, we present as Algorithm 3 the efficient **wn**-PiP algorithm documented in (Sunday, 2021, pp. 44–45). Here, we incorporated an extra boundary-point test.

5 Test cases

We design two types of test cases. In the first type, a test point $Q \in S^2$ lies on the extension of some side of the spherical n -gon G . In the second type, the curve winds around Q multiple times. We run the rotation-based reduction and shearing-based reduction for each test.

5.1 Antipode of test point is a boundary point

Type I. Let $Q(0, 0)$ be the north pole, and G be the spherical polygon with vertices $v_1(\frac{\pi}{2}, 0)$, $v_2(\pi, 0)$, and $v_3(\frac{\pi}{2}, \frac{\pi}{2})$. Note that G is a closed octant, and is thus AE per Definition 2.5. Because $-Q = v_2 \in G$, we must have $Q \notin G$ by Definition 2.2. Results in Appendix A confirm so.

5.2 Test point is a boundary point

Type I. Let $Q(0, 0)$ be the north pole, and G be the spherical polygon with vertices $v_1(\frac{\pi}{6}, 0)$, $v_2(\frac{\pi}{4}, \frac{\pi}{2})$, and $v_3(\frac{\pi}{6}, \pi)$. Results in Appendix A indeed confirm that $Q \in \partial G$.

Algorithm 1 Reduction algorithm for spherical n -gons that satisfy the antipode-excluding property.

Require: $[x_i, y_i, z_i]^\top, i = 1, \dots, n$ \triangleright Cartesian coordinates of vertices of G

Require: (θ, ϕ) \triangleright Polar and azimuthal angles of Q

1: $\mathbf{k} \leftarrow [k_x, k_y, k_z]^\top \leftarrow [\sin \phi, -\cos \phi, 0]^\top$ \triangleright Axis of rotation

2: $\mathbf{K} \leftarrow \begin{bmatrix} 0 & -k_z & k_y \\ k_z & 0 & -k_x \\ -k_y & k_x & 0 \end{bmatrix}$ \triangleright Cross-product matrix

3: $\mathbf{R} \leftarrow \mathbf{I} + (\sin \theta)\mathbf{K} + (1 - \cos \theta)\mathbf{K}^2$ \triangleright Rodrigue's rotation (matrix form)

4: **for** $i = 1, \dots, n$ **do**

5: $[x'_i, y'_i, z'_i]^\top \leftarrow \mathbf{R}[x_i, y_i, z_i]^\top$ \triangleright May use $3 \times n$ matrix instead

6: **end for**

7: (State, i) \leftarrow Algorithm 3 with $[x'_i, y'_i]^\top, (i = 1, \dots, n)$ required \triangleright PiP

8: **if** State is $O \in \partial G'$ **then** \triangleright True if $\pm Q \in \partial G$

9: $j \leftarrow i + 1$ if $i < n$ and 1 if $i = n$ \triangleright Next vertex index, cyclic

10: $\bar{z} \leftarrow \frac{1}{2}(z'_i + z'_j)$ \triangleright Proposition 2.8

11: **if** $\bar{z} > 0$ **then** \triangleright Is said midpoint above z -axis?

12: **return** $(Q \in \partial G, i)$ \triangleright i -th side contains Q

13: **else**

14: **return** $(Q \notin G, \text{undefined})$ \triangleright i -th side contains $-Q$, apply AE

15: **end if**

16: **else if** State is $O \in \hat{G}'$ **then**

17: **return** $(Q \in \hat{G}, i)$ \triangleright i is **wn**

18: **else** \triangleright State is $O \notin G'$

19: **return** $(Q \notin G, i)$ \triangleright i is **wn**

20: **end if**

Algorithm 2 Shearing-based reduction algorithm for spherical n -gons that satisfy the antipode-excluding property.

Require: $[x_i, y_i, z_i]^\top$, $i = 1, \dots, n$ \triangleright Cartesian coordinates of vertices of G
Require: (a, b, c) \triangleright Cartesian coordinates of Q

- 1: **if** $|a| \geq |b|$ and $|a| \geq |c|$ **then** \triangleright Align with x -axis?
- 2: **for** $i = 1, \dots, n$ **do** $[x'_i, y'_i, z'_i]^\top \leftarrow [x_i, y_i - \frac{b}{a}x_i, z_i - \frac{c}{a}x_i]^\top$ \triangleright x -shearing
- 3: **end for**
- 4: **if** $a > 0$ **then** (State, i) \leftarrow Algorithm 3 with $[y'_i, z'_i]^\top$, ($i = 1, \dots, n$)
- 5: **else** (State, i) \leftarrow Algorithm 3 with $[z'_i, y'_i]^\top$, ($i = 1, \dots, n$)
- 6: **end if**
- 7: **else if** $|b| \geq |c|$ **then** \triangleright Align with y -axis?
- 8: **for** $i = 1, \dots, n$ **do** $[x'_i, y'_i, z'_i]^\top \leftarrow [x_i - \frac{a}{b}y_i, y_i, z_i - \frac{c}{b}y_i]^\top$ \triangleright y -shearing
- 9: **end for**
- 10: **if** $b > 0$ **then** (State, i) \leftarrow Algorithm 3 with $[z'_i, x'_i]^\top$, ($i = 1, \dots, n$)
- 11: **else** (State, i) \leftarrow Algorithm 3 with $[x'_i, z'_i]^\top$, ($i = 1, \dots, n$)
- 12: **end if**
- 13: **else** \triangleright Align with z -axis
- 14: **for** $i = 1, \dots, n$ **do** $[x'_i, y'_i, z'_i]^\top \leftarrow [x_i - \frac{a}{c}z_i, y_i - \frac{b}{c}z_i, z_i]^\top$ \triangleright z -shearing
- 15: **end for**
- 16: **if** $c > 0$ **then** (State, i) \leftarrow Algorithm 3 with $[x'_i, y'_i]^\top$, ($i = 1, \dots, n$)
- 17: **else** (State, i) \leftarrow Algorithm 3 with $[y'_i, x'_i]^\top$, ($i = 1, \dots, n$)
- 18: **end if**
- 19: **end if**
- 20: **if** State is $O \in \partial G'$ **then** \triangleright True if $\pm Q \in \partial G$
- 21: $j \leftarrow i + 1$ if $i < n$ and 1 if $i = n$ \triangleright Next vertex index, cyclic
- 22: **if** $[a, b, c][x'_i + x'_j, y'_i + y'_j, z'_i + z'_j]^\top > 0$ **then** \triangleright Proposition 2.8
- 23: **return** $(Q \in \partial G, i)$ \triangleright i -th side contains Q
- 24: **else**
- 25: **return** $(Q \notin G, \text{undefined})$ \triangleright i -th side contains $-Q$, apply AE
- 26: **end if**
- 27: **else if** State is $O \in \overset{\circ}{G}$ **then**
- 28: **return** $(Q \in \overset{\circ}{G}, i)$ \triangleright i is **wn**
- 29: **else** \triangleright State is $O \notin G'$
- 30: **return** $(Q \notin G, i)$ \triangleright i is **wn**
- 31: **end if**

Algorithm 3 The **wn**-PiP algorithm adapted from (Sunday, 2021, pp. 44–45).

Require: $[x_i, y_i]^\top, i = 1, \dots, n$ \triangleright Coordinates of vertices of polygon G'

- 1: **wn** \leftarrow 0
- 2: **for** $i = 1, \dots, n$ **do**
- 3: $j \leftarrow i + 1$ if $i < n$ and 1 if $i = n$ \triangleright Next vertex index, cyclic
- 4: **if** $x_i y_j - y_i x_j = 0$ and $x_i x_j \leq 0$ **then** \triangleright Origin on the i -th edge?
- 5: **return** $(O \in \partial G', i)$ \triangleright Tags output with edge index
- 6: **end if**
- 7: **if** $y_i \leq 0$ **then**
- 8: **if** $y_j > 0$ **then**
- 9: **if** $x_i(y_j - y_i) - (x_j - x_i)y_i > 0$ **then**
- 10: **wn** \leftarrow **wn** + 1 \triangleright Crossing $+x$, CCW
- 11: **end if**
- 12: **end if**
- 13: **else**
- 14: **if** $y_j \leq 0$ **then**
- 15: **if** $x_i(y_j - y_i) - (x_j - x_i)y_i < 0$ **then**
- 16: **wn** \leftarrow **wn** - 1 \triangleright Crossing $+x$, CW
- 17: **end if**
- 18: **end if**
- 19: **end if**
- 20: **if** **wn** $>$ 0 **then**
- 21: **return** $(O \in \overset{\circ}{G'}, \mathbf{wn})$ \triangleright Tags output with winding number
- 22: **else**
- 23: **return** $(O \notin G', \mathbf{wn})$ \triangleright Tags output with winding number
- 24: **end if**
- 25: **end for**

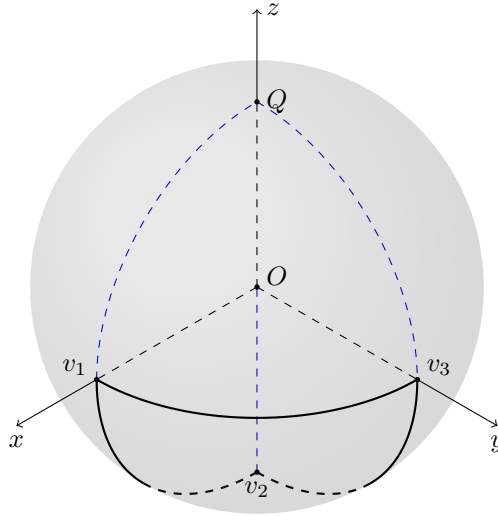


Figure 6: In test case 1, the test point is antipodal to a vertex of the spherical 3-gon. This 3-gon is a beloved equiangular right triangle.

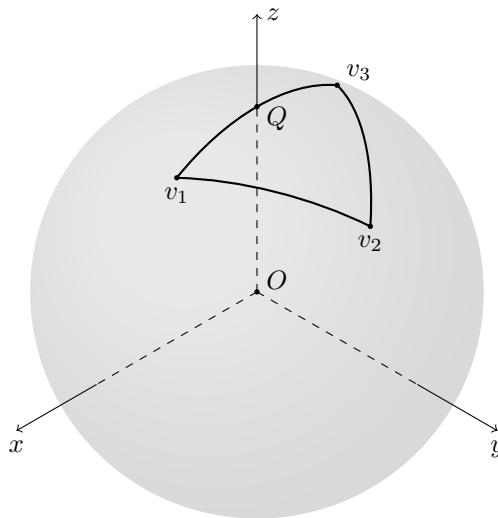


Figure 7: In test case 2, the test point falls in the interior of the third edge of an isosceles spherical 3-gon.

5.3 Non-simple yet orientable boundary

Type II. Let $Q(90^\circ, 45^\circ)$ be a point on the equator. We define G to be a non-simple spherical polygon defined using 10 vertices: $v_1(45^\circ, \arccos \frac{1}{8})$, $v_2(60^\circ, 30^\circ)$, $v_3(90^\circ, 0^\circ)$, $v_4(120^\circ, 30^\circ)$, $v_5(90^\circ, 60^\circ)$, $v_6 = v_1$, $v_7(90^\circ, 30^\circ)$, $v_8(120^\circ, 60^\circ)$, $v_9(90^\circ, 90^\circ)$, $v_{10}(60^\circ, 60^\circ)$. Results in Appendix A indeed confirm that $Q \in \overset{\circ}{G}$. Though not exposed, one may inspect the PiP algorithm to see that its winding number is indeed 2.

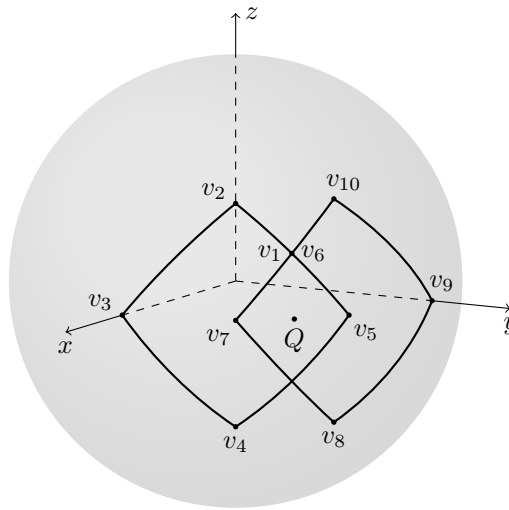


Figure 8: In test case 3, the test point falls in the interior of this non-simple spherical polygon. Count the spherical diamonds!

6 Discussion

We discuss a major concern during the development of the reduction algorithms. We then address the positioning of this work amongst prior work, end-user friendless, and offer some final conclusions.

6.1 Spherical lessons

Projections of spherical n -gons onto a plane are not necessarily polygons. The mismatch in homotopy classes between $(\pi \circ T)(G)$ and G' could easily

occur without careful choice of π and T . If π is homotopic to the south stereographic projection τ , then no mismatch will occur.

6.2 Interfacing with prior work

Because of the simplicity of **wn**, we second the opinion that **wn**-SPiP algorithms should be preferred over **cn**-SPiP algorithms, unless other factors are at play. Our algorithm makes no use of known interior points (KIP), but should one be known, it could be cached to enable other KIP-requiring **cn**-algorithms.

For batch testing, *i.e.*, multiple test points and multiple spherical polygons, note that the same test point induces the same rotation T , so a single test point could be matched against multiple spherical polygons at once. Recall that the rotation T is a linear transformation. We refrain from further complications and refer the reader to more recent developments in S^2 -friendly data structures, such as the SS-tree pioneered in White and Jain (1996).

6.3 User awareness

While this work makes no attempt to generalize into more general spherical polygons, attached code shown in Appendix A, provides documentation to alert users of a more friendly property (Definition 2.5) than BAE. This different emphasis could serve as a positive example for interfacing between package developers and users.

6.4 Conclusion

We have proposed a new reduction algorithm to transform the spherical point-in-polygon (SPiP) problem into the point-in-polygon (PiP) problem for boundary antipode-excluding (BAE) spherical polygons, a spherical n -gon whose boundary intersects trivially with its antipode. Spherical polygons fully contained within an open hemisphere is automatically BAE. Our reduction algorithms, rotation-based and shearing-based, preserve homotopy classes and passes specially designed test cases that could fail in prior work. We have successfully designed two winding-number (**wn**-)SPiP algorithms for BAE spherical polygons, both powered by an efficient **wn**-PiP algorithm,

References

- John R. Baumgardner and Paul O. Frederickson. Icosahedral discretization of the two-sphere. *SIAM Journal on Numerical Analysis*, 22(6):1107–1115, 1985.
- Michael Bevis and Jean-Luc Chatelain. Locating a point on a spherical surface relative to a spherical polygon of arbitrary shape. *Mathematical Geology*, 21(8):811–828, 1989.
- Allen Hatcher. *Algebraic Topology*. Cambridge University Press, 2001. ISBN 9780521795401.
- Ryan Ketzner, Vinay Ravindra, and Michael Bramble. A robust, fast, and accurate algorithm for point in spherical polygon classification with applications in geoscience and remote sensing. *Computers & Geosciences*, 167: 105185, 2022.
- Ziqiang Li. *Diffusion-Based Cartoglobes with Discrete Harmonic Transform and Spherical Finite Elements*. Dissertation, University of Wyoming, Laramie, WY, 2023.
- Ziqiang Li and Saman Aryana. Diffusion-based cartogram on spheres. *Cartography and Geographic Information Science*, 45(5):464–475, 2018. doi: 10.1080/15230406.2017.1408033.
- John P. Snyder. Map projections—a working manual. Technical report, US Government Printing Office, 1987.
- Daniel Sunday. *Practical Geometry Algorithms: with C++ Code*. Amazon KDP, 2021.
- Isaac Todhunter. *Spherical Trigonometry: For the Use of Colleges and Schools*. Macmillan, 5 edition, 1886.
- D. A. White and R. Jain. Similarity indexing with the SS-tree. In *Proceedings of the Twelfth International Conference on Data Engineering*, pages 516–523, 1996.

A Code Listings

The test cases are encoded in the test script below.

```
1 %% Test Case #1
2 % Test point Q is the north pole.
3 theta = 0;      % Polar angle; measured from north pole.
4 phi = 0;       % Azimuthal angle; measured from prime
   meridian.
5 G = [1  0  0; % Each column describes one vertex of G.
6      0  0  1;
7      0 -1  0];
8 [state,index] = spip(theta,phi,G); % Call SPiP.
9 % Expected state of -1 (exterior) and index of NaN.
10 fprintf('#1R: State %2d, Index %d.\n',state,index);
11 Q = [cos(theta) sin(theta)*cos(phi) sin(theta)*sin(phi)];
12 [state,index] = spipsh(Q,G); % Call SPiPsh
13 % Expected state of -1 (exterior) and index of NaN.
14 fprintf('#1S: State %2d, Index %d.\n',state,index);
15
16 %% Test Case #2
17 % Test point Q is the north pole, again.
18 theta = 0;
19 phi = 0;
20 G = [      1/2  0          -1/2 ; % G is AE.
21      0  1/sqrt(2)  0      ;
22      sqrt(3)/2  1/sqrt(2) sqrt(3)/2];
23 [state,index] = spip(theta,phi,G);
24 % Expected state of 0 (boundary) and index of 1.
25 fprintf('#2R: State %2d, Index %d.\n',state,index);
26 Q = [cos(theta) sin(theta)*cos(phi) sin(theta)*sin(phi)];
27 [state,index] = spipsh(Q,G);
28 fprintf('#2S: State %2d, Index %d.\n',state,index);
29
30 %% Test Case #3
31 % Test point Q is (90,45) in degrees.
32 theta = pi/2;
33 phi = pi/4;
34 G = [ 1/sqrt(2)  sqrt(3/8)  1/sqrt(8) ; % v1=v2v5 cap v7v10
35      3/4        sqrt(3)/4  1/2      ; % v2 ( 60,30)
36      1          0         0         ; % v3 ( 90, 0)
37      3/4        sqrt(3)/4 -1/2     ; % v4 (120,30)
38      1/2        sqrt(3)/2  0        ; % v5 ( 90,60)
39      1/sqrt(2)  sqrt(3/8)  1/sqrt(8) ; % v6=v1
40 sqrt(3)/2      1/2      0         ; % v7 ( 90,30)
41 sqrt(3)/4      3/4     -1/2     ; % v8 (120,60)
```

```

42     0          1      0          ; % v9 ( 90,90)
43 sqrt(3)/4      3/4    1/2      ]'; % v10( 60,60)
44 % Expected state of 1 (interior) and index of 2.
45 [state,index] = spip(theta,phi,G);
46 fprintf('#3R: State %2d, Index %d.\n',state,index);
47 Q = [sin(theta)*sin(phi) sin(theta)*cos(phi) cos(theta)];
48 [state,index] = spipsh(Q,G);
49 fprintf('#3S: State %2d, Index %d.\n',state,index);

```

The output below matches our expectation.

```

1 #1R: State -1, Index NaN.
2 #1S: State -1, Index NaN.
3 #2R: State 0, Index 3.
4 #2S: State 0, Index 3.
5 #3R: State 1, Index 2.
6 #3S: State 1, Index 2.

```

A.1 SPiP based on Rotation

```

1 %SPIP Spherical point-in-polygon (SPiP) problem.
2 % [S,I] = spip(theta,phi,G) determines if the test point Q
3 % with polar/azimuthal angle of theta/phi lies in the
4 % antipode-excluding (AE) spherical polygon G. Each column
5 % of G represents the Cartesian coordinates of a vertex.
6 % The sphere must be centered at the origin.
7 %
8 % If your spherical polygon is containable in an open
9 % hemisphere, congratulations!... as it is AE.
10 %
11 % Possible values of S:
12 %     1    Q is in the interior of G.
13 %     0    Q is on the boundary of G.
14 %    -1    Q is in the exterior of G.
15 %
16 % The index I is either: 1-based index of the first edge
17 % of G containing Q, or the winding number of Q around G.
18 function [S,I] = spip(theta,phi,G)
19     kx = sin(phi);
20     ky = -cos(phi);
21     K = [ 0  0  ky ; % Rodrigue's with kz=0.
22          0  0 -kx ;
23          -ky kx  0 ];
24     R = eye(3)+sin(theta).*K+(1-cos(theta)).*(K^2);
25     v_rot = R*G; % Q-north rotation.

```

```

26 % Call the PiP algorithm.
27 [S,I] = pip(v_rot(1,:),v_rot(2,:));
28 if S == 0
29     n = size(G,2);
30     if I<n
31         J = I+1;
32     else
33         J = 1;
34     end
35     zbar = (v_rot(3,I)+v_rot(3,J))/2;
36     if zbar < 0
37         S = -1;
38         I = NaN;
39     end
40 end
41 end

```

A.2 SPiP based on Shearing

```

1 %SPIPSH SPiP problem with shearing reduction.
2 % [S,I] = spipsh([x y z],G) determines if the test point
3 % Q(x,y,z) lies in the antipode-excluding (AE) spherical
4 % polygon G. Each column of G represents the Cartesian
5 % coordinates of a vertex. The sphere must be centered at
6 % the origin.
7 %
8 % If your spherical polygon is containable in an open
9 % hemisphere, congratulations!... as it is AE.
10 %
11 % Possible values of S:
12 %     1    Q is in the interior of G.
13 %     0    Q is on the boundary of G.
14 %    -1    Q is in the exterior of G.
15 %
16 % The index I is either: 1-based index of the first edge
17 % of G containing Q, or the winding number of Q around G.
18 function [S,I] = spipsh(Q,G)
19     a = Q(1);    b = Q(2);    c = Q(3);
20     X = G(1,:); Y = G(2,:); Z = G(3,:);
21     if max(abs(Q)) == abs(a)
22         if a>0
23             [S,I] = pip(Y-X*b/a,Z-X*c/a);
24         else
25             [S,I] = pip(Z-X*c/a,Y-X*b/a);
26         end

```

```

27     elseif max(Q) == abs(b)
28         if b>0
29             [S,I] = pip(Z-Y*c/b,X-Y*a/b);
30         else
31             [S,I] = pip(X-Y*a/b,Z-Y*c/b);
32         end
33     elseif max(Q) == abs(c)
34         if c>0
35             [S,I] = pip(X-Z*a/c,Y-Z*b/c);
36         else
37             [S,I] = pip(Y-Z*b/c,X-Z*a/c);
38         end
39     end
40     if S == 0
41         n = size(G,2);
42         if I<n
43             J = I+1;
44         else
45             J = 1;
46         end
47         if dot([a,b,c],[X(I)+X(J),Y(I)+Y(J),Z(I)+Z(J)])>0
48             S = -1;
49             I = NaN;
50         end
51     end
52 end

```

A.3 Sunday's efficient wn-PiP algorithm with modification

```

1 %PIP Point-in-polygon (PiP) problem.
2 % [S,I] = spip(X,Y) determines if the origin (0,0) lies in
3 % a polygon G. X and Y are vectors containing the
4 % Cartesian coordinates of vertices of G.
5 %
6 % Possible values of S:
7 %     1    Q is in the interior of G.
8 %     0    Q is on the boundary of G.
9 %    -1    Q is in the exterior of G.
10 %
11 % The index I is the 1-based index of the first edge of G
12 % that Q lies on. When Q is 1 or -1, I is meaninglessly 0.
13 %
14 % Reference: Sunday (2021)
15 function [S,I] = pip(X,Y)

```

```

16     wn = 0;
17     n = length(X);
18     I = 0;
19     for i = 1:n
20         if i<n
21             j = i+1;
22         else
23             j = 1;
24         end
25         % Q-on-side judgement.
26         if X(i)*Y(j)-Y(i)*X(j)==0 && X(i)*X(j)<=0
27             S = 0;
28             I = i;
29             return
30         end
31         if Y(i)<=0
32             if Y(j)>0
33                 if isLeft(X(i),Y(i),X(j),Y(j)) > 0
34                     wn = wn+1;
35                 end
36             end
37         else
38             if Y(j)<=0
39                 if isLeft(X(i),Y(i),X(j),Y(j)) < 0
40                     wn = wn-1;
41                 end
42             end
43         end
44     end
45     if wn>0
46         S = 1;
47     else
48         S = -1;
49     end
50     I = wn;
51 end
52
53 %ISLEFT Is the origin 0 to the left of the vector AB?
54 % a = isLeft(x1,y1,x2,y2) calculates the signed area of the
55 % triangle OAB specified by A(x1,y1) and B(x2,y2).
56 %
57 % Sign of a:
58 % If a is positive, then 0 is left of vector AB.
59 % If a is zero, then 0 and vector AB are collinear.
60 % If a is negative, then 0 is right of vector AB.

```



```
61 %  
62 % Reference: Sunday (2021)  
63 function area = isLeft(x1,y1,x2,y2)  
64     area = x1*(y2-y1)-(x2-x1)*y1;  
65 end
```